EXPERIMENTAL ARTICLES

UDC 577.175.8, 577.175.8, 612.3/.8 : 577 : 57.02 : 502/504
https://doi.org/10.15407/biotech17.06.005

AMINO-GRAFTED MESOPOROUS SILICA NANOPARTICLES: ASSESSMENT OF NEUROMODULATORY, MEMBRANOTROPIC AND ANTIOXIDANT PROPERTIES IN CORTEX NERVE TERMINALS

S.O. Sotnik[1]
I.M. Pavliei[1]
O.O. Pariiska[1]
Y.I. Kurys[1]
M.V. Dudarenko[2]
A.A. Borysov[2]
N.V. Krisanova[2]
N.G. Pozdnyakova[2]
L.M. Kalynovska[2]
M.M. Driuk[2]
A.O. Pastukhov[2]
A.S. Tarasenko[2]
V.G. Koshechko[1]
S.V. Kolotilov[1]
T.A. Borisova[2]

[1] L.V. Pisarzhevskii Institute of Physical Chemistry of the National Academy of Sciences of Ukraine, Kyiv

[2] O.V. Palladin Institute of Biochemistry of the National Academy of Sciences of Ukraine, Kyiv

E-mail: tborisov@biochem. kiev.ua

Received 2024/11/11
Revised 2024/11/25
Accepted 2024/11/26

Aim. In biomedical applications, silica nanoparticles are promising for controlled drug delivery. Also, from an environmental point of view, silica accounts for the most significant part of the mass of air pollution, particularly matter components, especially during sand dust storms.

Methods. Amino-grafted **m**esoporous **s**ilica **n**anoparticles (MSN-NH_2) were synthesized by means of co-condensation of tetraethoxysilane and 3-aminopropyltriethoxysilane and characterized using TEM, SEM, FTIR-spectroscopy, and powder X-ray diffraction. Neuromodulatory and related properties of MSN-NH_2 were evaluated using rat cortex nerve terminals (synaptosomes).

Results. MSN-NH_2 did not influence the extracellular synaptosomal level of excitatory neurotransmitter L-[^{14}C]glutamate and so did not cause excitotoxicity. In fluorescence measurements, MSN-NH_2 depolarised the synaptosomal membrane and demonstrated weak antioxidant properties, decreasing the spontaneous generation of reactive oxygen species, whereas MSN-NH_2 did not alter H_2O_2 in nerve terminals. The model of Cd^{2+}/Pb^{2+}/Hg^{2+}-induced excitotoxicity was used to assess the capability of MSN-NH_2 to adsorb xenobiotic heavy metals. MSN-NH_2 did not modulate the Cd^{2+}/Pb^{2+}/Hg^{2+}-induced increase in the extracellular synaptosomal level of L-[^{14}C]glutamate.

Conclusions. MSN-NH_2 did not demonstrate excitotoxic signs, had weak antioxidant properties, and was biocompatible. MSN-NH_2 did not mitigate the excitotoxic effects of xenobiotic heavy metals and did not adsorb these metals in biological systems.

Key words: mesoporous amino-grafted silica nanoparticles, neuromodulatory, membranotropic, antioxidant properties, xenobiotic heavy metals, glutamate, cortex nerve terminals.

Mesoporous silica nanoparticles (MSN), due to their tunable structure, various surface functionalization properties, and exceptional biocompatibility, are acknowledged as a principal example of nanotechnology applied in the biomedical fields. MSNs are progressively moving from basic research to clinical trials. A wide variety of MSN-based nanoplatforms was developed over the past two decades through design and controlled preparation techniques, demonstrating their adaptability to diverse biomedical applications, in particular with the breakthroughs in the fields of biosensing, tissue engineering, disease diagnosis, and treatment, etc. [1]. MSN are promising as nanocarriers for efficient site-specific delivery of highly toxic drugs, in particular for cancer treatment [2].

Also, from an environmental point of view, silica accounts for the most significant part of the mass of air pollution, particulate matter components, especially during sand dust storms. Silica particles, due to their specific physical and chemical properties, structure, and composition, can adsorb toxic pollutants in the environment. The WHO toxicology review of real-world exposures has revealed that sand dust particles collected from surface soils and dust-storm particles sampled at remote locations mixed with industrial pollutants induced inflammatory lung injury [3, 4]. Airborne particulate matter can reach the nervous system of humans and trigger the development of neurological and neurodegenerative disorders/diseases [5–7].

The aims of this study were (i) to synthesize amino-grafted **m**esoporous **s**ilica **n**anoparticles (MSN-NH_2) by means of co-condensation of tetraethoxysilane (silica source, TEOS) with 3-aminopropyltriethoxysilane (source of amino-groups, APTES) in the presence of template — cetyltrimethylammonium bromide (CTAB), and characterise them using transmission (TEM) and scanning (SEM) electron microscopy, Fourier transform infrared spectroscopy (FTIR) and X-ray diffraction; (ii) to analyse their biocompatibility by monitoring neuromodulatory, membranotropic and oxidative properties in isolated cortex nerve terminals (synaptosomes), in particular the extracellular level of the primary excitatory neurotransmitter L-[^{14}C] glutamate, the membrane potential, generation of reactive oxygen species (ROS), including hydrogen peroxide; to evaluate xenobiotic heavy metal adsorption capability of MSN-NH_2 using a model of acute Cd^{2+}/Pb^{2+}/Hg^{2+}-induced excitotoxicity in nerve terminals. It should be noted that synaptosomes are the best model to study the presynaptic processes [8]. It could be expected that the presence of NH_2-groups on the surface of MSN would facilitate the binding of heavy metal ions. Importantly, impaired transport of glutamate in the presynaptic nerve terminals provokes presynaptic malfunction and the development of neuropathology and is involved in the pathogenesis of neurological and neurodegenerative disorders and diseases.

Materials and Methods

HEPES, EGTA, EDTA, Ficoll 400, High-Performance LSC Cocktail, salts of the analytical grade were obtained from Sigma, USA; L-[^{14}C] glutamate — Perkin Elmer, Waltham, MA, USA. The high-purity graphite rods (99.9995%) were obtained from Alfa Aesar. Tetraethoxysilane (TEOS), cetyltrimethylammonium bromide (CTAB), and 3-aminopropyltriethoxysilane (APTES) were purchased from Enamine Ltd.

Synthesis of amino-grafted mesoporous silica nanoparticles

MSN-NH_2 particles were obtained by co-condensation of TEOS and APTES followed by treatment with hydrochloric acid in methanol for 16 hours according to a published procedure [9]. Namely, 0.7 g (1.9 mmol) of CTAB was added to a mixture of 336 ml of distilled water and 2.45 ml of 2M NaOH, and the reaction mixture was heated to 80 °C. Then, 3.5 ml (15.8 mmol) of TEOS and 0.44 ml of APTES (1.88 mmol) were added simultaneously (1 drop of APTES for every 4 drops of TEOS). The mixture was then stirred at 1200 rpm at 80 °C for 2h, filtered, washed with 500 ml of 50/50 volume % ethanol/water mixture, and dried at 60 °C for 24h. For elimination of template (CTAB), the solid was placed in 100 ml of methanol with 5 drops of 37.5% HCl for 16 h with continuous stirring, then centrifuged at 6000 rpm for 15 minutes and dried at 60 °C overnight, then ground fine and dried for 6h more at 60 °C. The yield of MSN-NH_2 was 0.873 g.

Rats and Ethics

All animal-involving procedures were performed in accordance with the guidelines of the European Community (2010/63/EU), "Scientific Requirements and Research Protocols", "Research Ethics Committees" of the Declaration of Helsinki, and "ARRIVE guidelines for reporting experiments involving animal" [10, 11]; and also local Ukrainian laws and policies. Animals, Wistar rats, males,

3 months' of age, were retained in the vivarium of Palladin Institute of Biochemistry of the National Academy of Sciences of Ukraine, in a quiet and temperature-controlled room at 22–23 °C. Animals were provided with dry food pellets and water *ad libitum*. The experimental protocols were approved by the Animal Care and Use Committee of Palladin Institute of Biochemistry (Protocol No. 1 from 2024/02/16). The total number of animals was 9.

Isolation of the synaptosomes from the rat cortex

Nerve terminals were isolated from the cortex regions of the rat brain. The cortex regions were removed and homogenized in the following ice-cold solution: sucrose 0.32 M; HEPES-NaOH 5 mM, pH 7.4; EDTA 0.2 mM. One synaptosome preparation was obtained from one rat. Isolation procedures were conducted at + 4 °C. The synaptosomes were obtained according to the Cotman method with minor modifications [12, 13] by differential/Ficoll-400 density gradient centrifugation. The synaptosomes were appropriate for experiments for 2–4 hours after isolation. The standard saline solution contained: NaCl 126 mM; KCl 5 mM; $MgCl_2$ 2.0 mM; NaH_2PO_4 1.0 mM; HEPES 20 mM, pH 7.4; and D-glucose 10 mM. Protein concentrations were monitored according to Larson [14].

The extracellular synaptosomal level of L-[^{14}C] glutamate

The synaptosomes were diluted up to a concentration of 2 mg of protein/ml, and then they were pre-incubated at 37 °C for 10 min and loaded with L-[^{14}C] glutamate (1 nmol per mg of protein, 238 mCi/mmol) at 37 °C for 10 min. The synaptosomes, after loading, were washed with 10 volumes of the ice-cold standard saline solution and centrifuged (10.000×g, 20 s) at +4 °C; the pellets were re-suspended in the standard saline solution (up to 1 mg protein/ml). The extracellular level of L-[^{14}C] glutamate was assessed in the synaptosome preparations (125 µl, 0.5 mg of protein/ml). The synaptosome aliquots were pre-incubated for 8 min to restore the ion gradients. Then MSN-NH_2, Cd^{2+} (1 mM $CdCl_2$), Pb^{2+} (2.5 mM Pb acetate (PbAc)), and Hg^{2+} (5 µM $HgCl_2$) were added to the synaptosomes, and further they were incubated at 37 °C for 0 min and 15 min, and then were centrifuged at 10.000×*g* for 20 s at room temperature. The L-[^{14}C] glutamate values were monitored in the supernatant aliquots (100 µl), and the pellets were preliminary treated with SDS (100 ml of 10% SDS stock solution) using the scintillation cocktail High Performance LSC Cocktail (1.5 ml) and liquid scintillation counter Hidex 600SL (Finland) [15]. The experimental data were collected from "n" independent experiments carried out in triplicate using different synaptosome preparations.

The synaptosomal membrane potential

The synaptosomal membrane potential was recorded using the fluorescent potentiometric dye rhodamine 6G (0.5 µM) based on its potential-dependent binding to the membrane. Synaptosomes (0.2 mg of protein per ml) were pre-incubated at 37 °C for 10 min in a thermostated cuvette. Synaptosomes were equilibrated with the dye, and then MSN-NH_2 were added. The ratio (F), the index of the membrane potential, was calculated according to the equation F = Ft / F0, where F0 and Ft were the fluorescence intensity of the probe in the absence and presence of synaptosomes, respectively. F0 was evaluated by extrapolation of the exponential decay function to t = 0. Fluorescence measurements were performed using a fluorescence spectrofluorimeter Hitachi 650-10S at 528 nm (excitation) and 551 nm (emission) wavelengths.

Spontaneous ROS generation in nerve terminals

2′,7′-dichlorodihydro-fluoresceindiacetate (H2-DCFDA), a cell-permeable non-fluorescent probe, was used to record ROS production in nerve terminals. The dye became fluorescent upon oxidation after the de-esterification in the intracellular space. Synaptosomes with a concentration of 0.2 mg of protein/ml were pre-incubated with H2-DCFDA at a concentration of 5 µM in a stirring thermostated cuvette at 37 °C for 3 min. Then, the kinetic measurements were carried out. Changes in 2′,7′-dichlorofluorescein (DCF) fluorescence were monitored at excitation 502 nm and emission 525 nm wavelengths, slit bands were 2 nm each, using a fluorescence spectrofluorimeter QuantaMasterTM 40 (PTI, Inc., Canada).

Spectrophotometry measurements of H_2O_2 level in nerve terminals

The classical method for monitoring hydrogen peroxide concentrations through direct measurement of the absorbance at 240 nm was applied. In addition, hydrogen peroxide concentrations were measured based on the reaction of hydrogen peroxide with ammonium molybdate to produce a yellowish color, which

has a maximum absorbance at 374 nm [16]. The measurements were performed using spectrophotometer Shimadzu UV-1900i.

Statistical analysis

The experimental data were expressed as the mean ± S.E.M. of n independent experiments. One-way and two-way ANOVA were applied; the accepted significance level was $P < 0.05$. Two-way ANOVA followed by Tukey's post hoc test was applied to assess the interactions between MSN-NH_2 and Cd^{2+}, Pb^{2+}, and Hg^{2+} (MSN-NH_2 treatment and Cd^{2+}/Pb^{2+}/Hg^{2+} treatment were the independent factors).

Results and Discussion

Characterization of amino-grafted mesoporous silica nanoparticles

The MSN-NH_2 were obtained by co-condensation of TEOS with APTES (source of amino-groups, APTES) in the presence of template — cetyltrimethylammonium bromide (CTAB).

Amino-groups originated from APTES; TEOS served as a source of additional silica, while CTAB played the role of template, providing for the porous structure of the nanoparticles. Co-condensation method provides for more uniform distribution of amino groups on the surface of particles compared to post-synthetic grafting [9].

According to TEM results, the MSN-NH_2 were beans-shaped with a linear length of 400 nm and width of 200 nm (Fig.1, *A*). These results do not agree with the reported images for similar particles, where spherical particles with an average diameter of about 140–170 nm were reported [9]. In addition, oblong oval particles were visualized on the SEM image (Fig. 1, *B*).

The presence of nitrogen and carbon in MSN-NH_2 was confirmed by energy dispersive X-Ray analysis. It was found that MSN-NH_2 contained 2.8 % of nitrogen, 35.6% of carbon, 16.6% of silicon and 45% of oxygen. High carbon content could indicate the presence of residual CTAB in the sample, probably as cetyltrimethylammonium hydroxide, since the elemental composition of the particles obtained does not contain bromine atoms. Nevertheless, at least 0.6% of the nitrogen comes from APTES, indicating that aminofunctionalization of MSN was successful.

There were weak absorption bands at 3300 cm^{-1} and 1634 cm^{-1} in the FTIR spectrum of MSN-NH_2, which correspond to the stretching and deformation vibrations of the amino group (Fig. 2). The bands corresponding to the stretching symmetric and antisymmetric vibrations of the C–H bonds of the methylene groups of the aminopropyl chains and CTAB fragments were observed at 2853 cm^{-1} and 2928 cm^{-1}, respectively. All these bands were consistent with the presence of aminopropyl groups in MSN-NH_2.

The stretching, scissoring, and rocking deformation vibrations of the silanol bonds were observed at 1037 cm^{-1}, 798 cm^{-1}, and 452 cm^{-1}. The broad shoulder at 1140 cm^{-1} corresponded to the stretching vibrations of the Si-O bonds [17, 18]. The absorption band at 963 cm^{-1} could be assigned to asymmetric stretching vibrations of SiOH groups and indicated their presence in the MSN-NH_2 sample [19].

Low-angle reflections specific to the MCM-41 porous structure were observed in the diffraction pattern of the MSN-NH_2 sample (Fig. 3). The low intensity of the (110) and (200) peaks could be associated with the inclusion of functional groups in the pores of MSN (Fig. 3) [9].

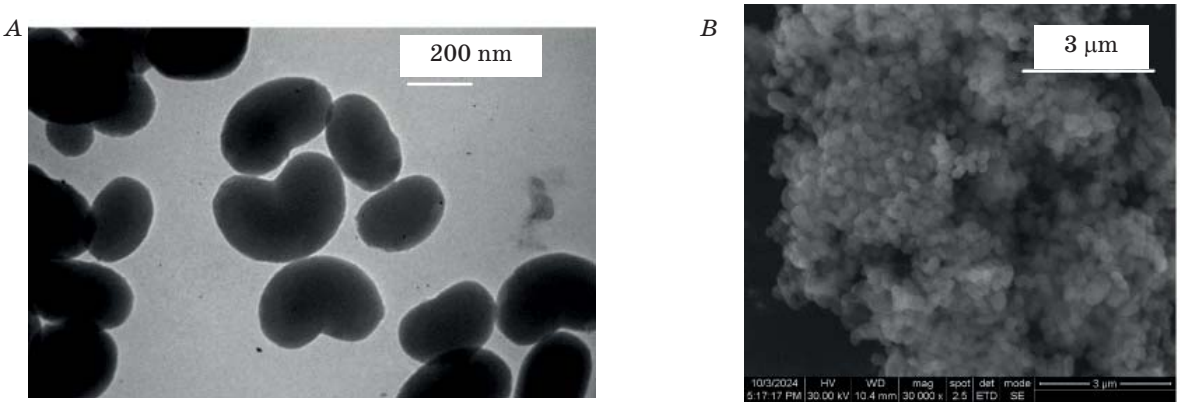

Fig. 1. **TEM (*A*) and SEM (*B*) images of MSN-NH_2**

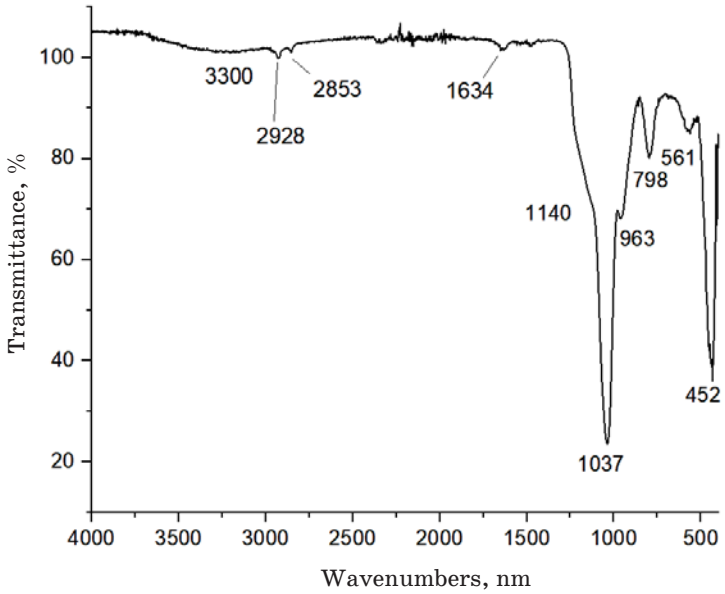

Fig. 2. **IR-spectrum of MSN-NH_2**

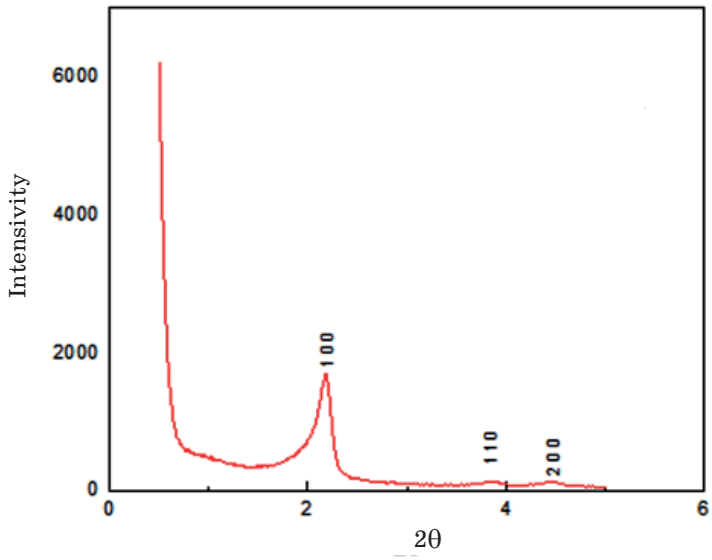

Fig. 3. **X-ray diffraction pattern of MSN-NH_2**

The extracellular level of L-[^{14}C] glutamate in nerve terminal preparations in the presence of MSN-NH_2

The extracellular level of glutamate represents a balance of transporter-mediated uptake of glutamate and its unstimulated release [20, 21]. As shown in Table 1, MSN-NH_2 did not change the extracellular synaptosomal level of L-[^{14}C] glutamate within the concentration range of 0.1–1.0 mg/ml. Therefore, MSN-NH_2 did not possess excitotoxic signs and was biocompatible.

Effect of MSN-NH_2 on the membrane potential of nerve terminals

The membrane potential of nerve terminals is a driving force of transporter-mediated uptake and release of glutamate and also reproduces the membrane integrity. The synaptosomal membrane potential was monitored using potentiometric fluorescent dye rhodamine 6G (see Method section). The standard saline solution added to the synaptosomal incubation was considered as a control. As shown in Fig. 4, the application of MSN-NH_2 at a concentration of 1.0 mg/ml caused membrane depolarization.

Table 1

The extracellular level of neurotransmitter L-[^{14}C] glutamate in the nerve terminal preparations in the presence of MSN-NH_2

	The extracellular level of L-[^{14}C] glutamate in nerve terminal preparations (% of total accumulated label)	**F; *p*-value**
Control	14.30 ± 0.17	
MSN-NH_2; 0.1 mg/ml	14.35 ± 0.21	$F_{(1,16)} = 0.03$; p = 0.86; n.s.
MSN-NH_2; 0.5 mg/ml	14.18 ± 0.25	$F_{(1,16)} = 0.18$; p = 0.67; n.s.
MSN-NH_2; 1.0 mg/ml	13.96 ± 0.23	$F_{(1,16)} = 1.64$; p = 0.22; n.s.
Note		

Note: Data are the mean ± SEM. n.s., no significant differences as compared to the control, $n = 9$.

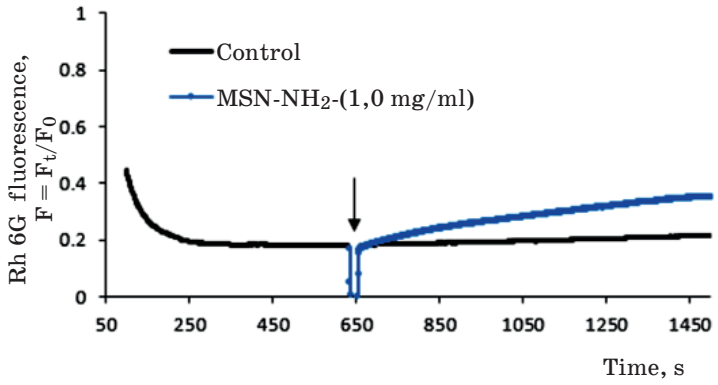

Fig. 4. **The membrane potential of nerve terminals in the presence of MSN-NH_2 at a concentration of 1.0 mg/ml**

Note. Synaptosomes were equilibrated with 0.5 μM rhodamine 6G, and when the steady level of the dye fluorescence was reached, the standard saline buffer or MSN-NH_2 was added to the synaptosomes (arrow). The trace is representative of 6 experimental data records performed with different synaptosomal preparations.

It should be noted that additional experiments without synaptosomes were carried out to monitor possible changes in rhodamine 6G fluorescence in the presence of MSN-NH_2. No changes in the dye fluorescence were revealed in these experiments, and no unspecific interaction of rhodamine 6G and MSN-NH_2 was found without synaptosomes.

However, taking into account the absence of effects of MSN-NH_2 on the extracellular level of L-[^{14}C] glutamate in nerve terminal preparation, further detailed studies are necessary in order to exclude the completely unspecific interaction of MSN-NH_2 and rhodamine 6G.

ROS generation in nerve terminals in the presence of MSN-NH_2

Kinetics of spontaneous ROS generation in the nerve terminals was monitored using fluorescent dye H2-DCFDA (see Method section). Figure 5 represents the effects of MSN-NH_2 on the spontaneous ROS generation, where it was demonstrated that MSN-NH_2 at concentrations of 10–20 microg/ml slightly decreased this parameter in nerve terminals.

Therefore, MSN-NH_2 at concentrations of 10–20 microg/ml revealed weak antioxidant properties in nerve terminals.

ROS-sensitive fluorescent dye H2-DCFDA (DCF, after the de-esterification, see Method section) (Fig. 5) is able to monitor all types of ROS generated in nerve terminals. To analyse individual ROS in synaptosomes,

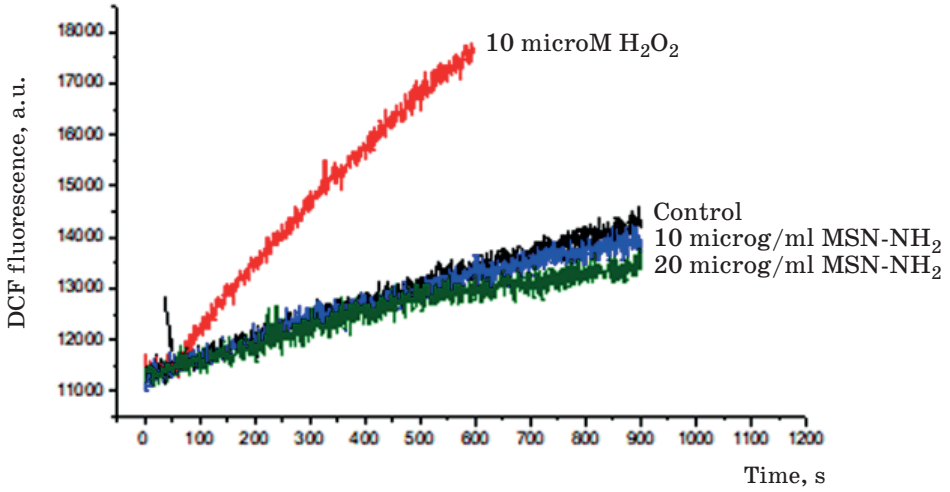

Fig. 5. **Spontaneous ROS generation in the nerve terminals in the presence of MSN-NH_2**
Note. The trace is representative of 6 experimental data records performed with different synaptosomal preparations.

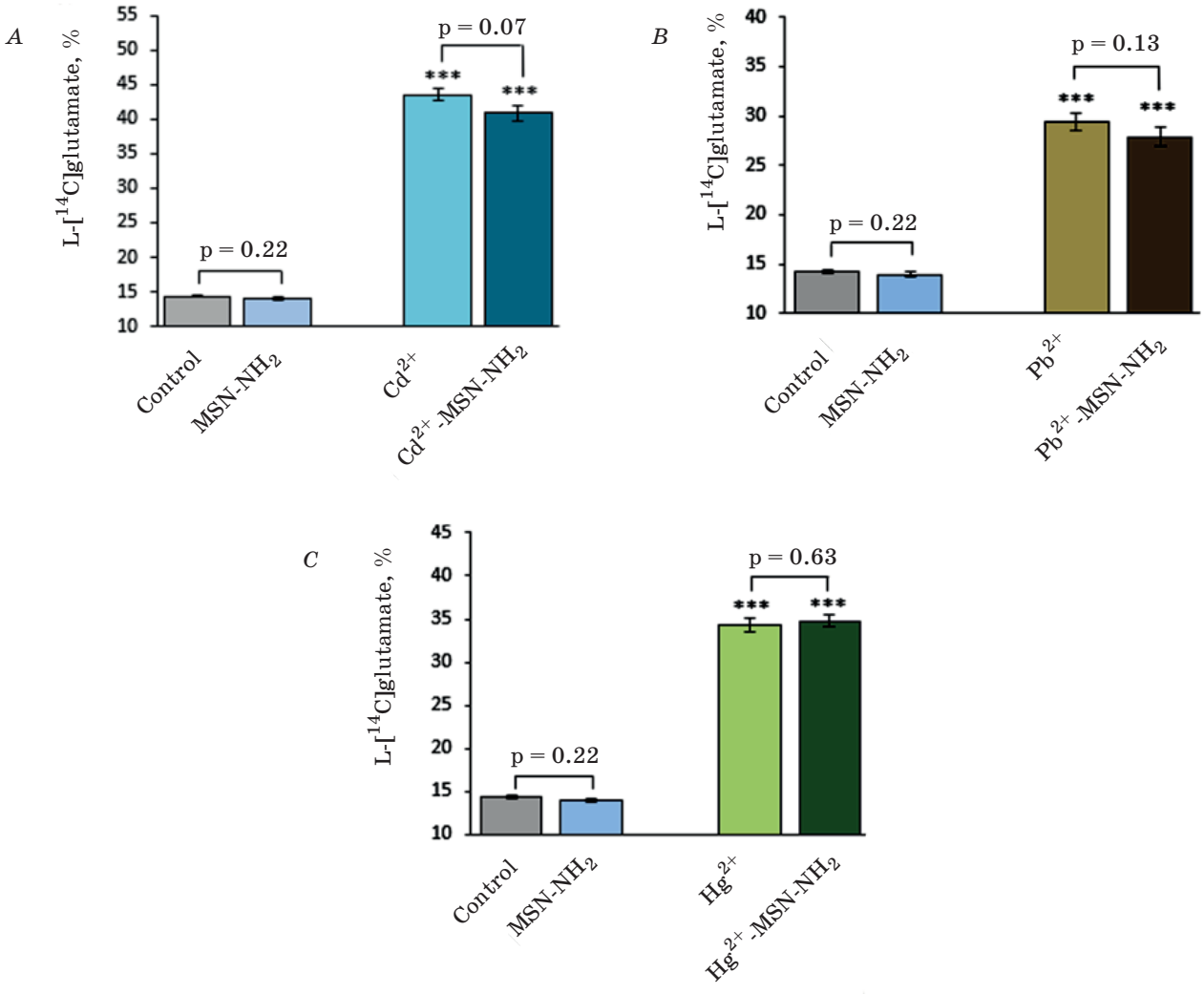

Fig. 6. **MSN-NH_2 (1.0 mg/ml) did not modulate an excitotoxic increase in the extracellular synaptosomal level of L-[^{14}C] glutamate induced by Cd^{2+} (*A*), Pb^{2+} (*B*), Hg^{2+} (*C*)**
Note. Data are the mean ± SEM. ***, $P < 0.001$; as compared to the control; $n = 9$.

the spectrophotometry experiments on the detection of one of the crucial components of ROS cohort, i.e. H_2O_2, were performed. The concentrations of H_2O_2 in nerve terminals were recorded using classical methods for monitoring H_2O_2 concentrations through direct measurement of its absorbance at 240 nm. In addition, H_2O_2 concentrations were measured at 374 nm based on the reaction of H_2O_2 with ammonium molybdate [16]. It was revealed using both methodical approaches that the addition of MSN-NH_2 to the synaptosomes did not change H_2O_2 spontaneously generated in the nerve terminals. These results were in accordance with the above fluorescent experiments using DCF.

Assessment of the capability of MSN-NH_2 to modulate excitotoxicity induced by xenobiotic heavy metals

In this set of experiments, the capability of MSN-NH_2 to modulate Cd^{2+}/Pb^{2+}/Hg^{2+}-induced increase in the extracellular level of L-[^{14}C] glutamate in nerve terminals was analysed. MSN-NH_2 and Cd^{2+}, Pb^{2+}, or Hg^{2+} were mixed and pre-incubated for 30 min before the addition to synaptosomes.

As shown in Fig. 6, MSN-NH_2 at a concentration of 1.0 mg/ml did not change excitotoxic Cd^{2+}/Pb^{2+}/Hg^{2+}-induced increase in the synaptosomal extracellular level of L-[^{14}C] glutamate.

Therefore, MSN-NH_2 was inert regarding mitigation or aggravation of Cd^{2+}/Pb^{2+}/Hg^{2+}-induced excitotoxic effects in nerve terminals.

Two-way ANOVA revealed no interaction between Cd^{2+} and MSN-NH_2 [$F_{(1,32)}$ = 2.68; p = 0.11; n = 9], between Pb^{2+} and MSN-NH_2 [$F_{(1,32)}$ = 2.85; p = 0.10; n = 9] and between Hg^{2+} and MSN-NH_2 [$F_{(1,32)}$= 0.64; p = 0.43; n = 9] in L-[^{14}C] glutamate experiments.

Conclusions

MSN-NH_2, synthesized by means of co-condensation of tetraethoxysilane and 3-aminopropyltriethoxysilane, did not influence the extracellular synaptosomal level of L-[^{14}C] glutamate, demonstrated weak antioxidant properties, decreasing spontaneous ROS generation, did not alter hydrogen peroxide generated in nerve terminals, whereas depolarised the synaptosomal membrane. MSN-NH_2 was inert regarding mitigation or aggravation of Cd^{2+}/Pb^{2+}/Hg^{2+}-induced excitotoxicity in nerve terminals. Therefore, MSN-NH_2 did not possess excitotoxicity signs, is biocompatible, and did not modulate excitotoxicity induced by xenobiotic heavy metals in biological systems.

Funding

This work was supported by the National Research Foundation of Ukraine: NRFU grant No. 2021.01/0061 “Cumulative neurotoxic effect of multicomponent pollution by airborne particles and neuroactive pharmaceuticals, biomaterials (including SARS-CoV-2), toxic metals and its prevention”.

Competing interests

The authors declare no financial and non-financial competing interests existed.

Authors’ contribution

Authors contributions: MSN-NH_2 synthesis and characterisation — SS, IP, OP, YK; synaptosome preparations were obtained by AP, MMD, LK; L-[^{14}C] glutamate and fluorimetry experiments — MVD, NP, NK AB, AP, AT; data analysis and figure preparation — SS, OP, MVD, AP, TB, SK; funding acquisitions, project leading, data analysis and paper writing — SS, TB, VK, SK.

REFERENCES

1. *Xu B., Li S., Shi R., Liu H.* Multifunctional mesoporous silica nanoparticles for biomedical applications. *Signal Transduct Target Ther.* 2023, 8(1): 1–28. https://www.nature.com/articles/s41392-023-01654-7
2. *Vallet-Regí M., Colilla M., Izquierdo-Barba I., Manzano M.* Mesoporous silica nanoparticles for drug delivery: Current insights. *Molecules.* 2018, 23(1): 47. https://pubmed.ncbi.nlm.nih.gov/29295564/
3. *Liu H., Wang X., Talifu D., Ding X., Abulizi A., Tursun Y., An J., Li K., Luo P., Xie X.* Distribution and sources of PM2.5-bound free silica in the atmosphere of hyper-arid regions in Hotan, North-West China. *Sci Total Environ.* 2022, 810:152368. https://doi.org/10.1016/j.scitotenv.2021.152368.
4. *WHO.* Sand and dust storms. 2024. https://www.who.int/news-room/fact-sheets/detail/sand-and-dust-storms
5. *Landrigan P.J., Fuller R., Acosta N.J.R., et al.* The Lancet Commission on pollution and health. *Lancet.* 2018, 391(10119): 462–512. https://doi.org/10.1016/S0140-6736(17)32345-0

6. *Borisova T.* Nervous System Injury in Response to Contact With Environmental, Engineered and Planetary Micro- and Nano-Sized Particles. *Front Physiol*. 2018, 9: 728. https://www.frontiersin.org/article/10.3389/fphys.2018.00728/full
7. *Tranvik L.J.* New light on black carbon. *Nat Geosci*. 2018, 11(8): 547–548. https://doi.org/10.1038/s41561-018-0181-x
8. *Sudhof T.C.* The synaptic vesicle cycle. *Annu Rev Neurosci*. 2004, 27: 509–547. https://doi.org/10.1146/annurev.neuro.26.041002.131412
9. *Estevão B.M., Miletto I., Hioka N., Marchese L., Gianotti E.* Mesoporous silica nanoparticles functionalized with amino groups for biomedical applications. *ChemistryOpen*. 2021, 10: 1251–1259. https://doi.org/10.1002/open.202100227
10. *Kilkenny C., Browne W., Cuthill I.C., Emerson M., Altman D.G.* NC3Rs Reporting Guidelines Working Group. Animal research: reporting in vivo experiments: the ARRIVE guidelines. *Br. J. Pharmacol*. 2010, 160(7): 1577–1579. http://www.ncbi.nlm.nih.gov/pubmed/20649561
11. *McGrath J.C., Drummond G.B., McLachlan E.M., Kilkenny C., Wainwright C.L.* Guidelines for reporting experiments involving animals: the ARRIVE guidelines. *Br. J. Pharmacol*. 2010, 160(7): 1573–1576. http://www.ncbi.nlm.nih.gov/pubmed/20649560
12. *Cotman C.W.* Isolation of synaptosomal and synaptic plasma membrane fractions. *Methods Enzymol*. 1974, 31: 445–452. http://www.ncbi.nlm.nih.gov/pubmed/4278474
13. *Krisanova N., Pozdnyakova N., Pastukhov A., Dudarenko M., Maksymchuk O., Parkhomets P., Sivko R., Borisova T.* Vitamin D3 deficiency in puberty rats causes presynaptic malfunctioning through alterations in exocytotic release and uptake of glutamate/GABA and expression of EAAC-1/GAT-3 transporters. *Food Chem. Toxicol*. 2019, 123: 142–150. https://linkinghub.elsevier.com/retrieve/pii/S0278691518307944
14. *Larson E., Howlett B., Jagendorf A.* Artificial reductant enhancement of the Lowry method for protein determination. *Anal. Biochem*. 1986, 155(2): 243–248. https://doi.org/10.1016/0003-2697(86)90432-X
15. *Pozdnyakova N., Pastukhov A., Dudarenko M., Galkin M., Borysov A., Borisova T.* Neuroactivity of detonation nanodiamonds: dose-dependent changes in transporter-mediated uptake and ambient level of excitatory/inhibitory neurotransmitters in brain nerve terminals. *J. Nanobiotechnology*. 2016, 14(1): 25. http://jnanobiotechnology.biomedcentral.com/articles/10.1186/s12951-016-0176-y
16. *Hadwan M.H., Abed H.N.* Data supporting the spectrophotometric method for the estimation of catalase activity. *Data Br*. 2016, 6: 194–199. https://doi.org/10.1016/j.dib.2015.12.012
17. *Pai P.G., Chao S.S., Takagi Y., Lucovsky G.* Infrared spectroscopic study of SiOx films produced by plasma enhanced chemical vapor deposition. *J. Vac. Sci. Technol. A* 1986, 4: 689–694. https://doi.org/10.1116/1.573833
18. *Zhang B.-R., Yu Z., Collins G.J., Hwang T., Ritchie W.H.* Chemical composition of soft vacuum electron beam assisted chemical vapor deposition of silicon nitride/oxynitride films versus substrate temperature. *J. Vac. Sci. Technol. A* 1989, 7: 176–188. https://doi.org/10.1116/1.575749
19. *Méndez-Vivar J., Mendoza-Bandala A.* Spectroscopic study on the early stages of the polymerization of hybrid TEOS–RSi(OR′)3 Sols. *J. Non. Cryst. Solids*. 2000, 261: 127–136. https://doi.org/10.1016/S0022-3093(99)00605-5
20. *Borisova T., Borysov A.* Putative duality of presynaptic events. *Rev. Neurosci*. 2016, 27: 377–383. https://www.degruyter.com/view/j/revneuro.ahead-of-print/revneuro-2015-0044/revneuro-2015-0044.xml
21. *Borisova T., Borysov A., Pastukhov A., Krisanova N.* Dynamic gradient of glutamate across the membrane: glutamate/aspartate-induced changes in the ambient level of L-[(14)C]glutamate and D-[(3)H]aspartate in rat brain nerve terminals. *Cell Mol. Neurobiol*. 2016, 36(8): 1229–1240. http://www.ncbi.nlm.nih.gov/pubmed/26886753

МЕЗОПОРИСТІ НАНОЧАСТИНКИ КРЕМНЕЗЕМУ З ЗАКРІПЛЕНИМИ АМІНОГРУПАМИ: ОЦІНКА НЕЙРОМОДУЛЯТОРНИХ, МЕМБРАНОТРОПНИХ ТА АНТИОКСИДАНТНИХ ВЛАСТИВОСТЕЙ У НЕРВОВИХ ЗАКІНЧЕННЯХ КОРИ ГОЛОВНОГО МОЗКУ

С.О. Сотник[1], *І.М. Павлєй*[1], *О.О. Парійська*[1], *Я.І. Курись*[1], *М.В. Дударенко*[2], *А.А. Борисов*[2], *Н.В. Крисанова*[2], *Н.Г. Позднякова*[2], *Л.М. Калиновська*[2], *М.М. Дрюк*[2], *А.О. Пастухов*[2], *А.С. Тарасенко*[2], *В.Г. Кошечко*[1], *С.В. Колотілов*[1], *Т.О. Борисова*[2]

[1]Інститут фізичної хімії ім. Л.В.Писаржевського НАН України, Київ
[2]Інститут біохімії ім. О.В. Палладіна Національної академії наук України, Київ

E-mail: *tborisov@biochem. kiev.ua*

Мета. У біомедичному застосуванні наночастинки кремнезему є перспективними для контрольованої доставки ліків. З екологічної точки зору на кремнезем припадає найбільша частина маси окремих компонентів забруднення повітря, особливо під час піщаних пилових бурь.

Методи. Мезопористі кремнеземні наночастинки із закріпленими аміногрупами (MSN-NH_2) синтезовані шляхом ко-конденсації тетраетоксісілану і 3-амінопропілтриетоксісілану і охарактеризовані методами ТЕМ, ІЧ-спектроскопії та рентгенофазового аналізу. Нейромодулювальні та пов'язані з ними властивості MSN-NH_2 оцінювали у нервових закінченнях кори головного мозку щурів (синаптосомах).

Результати. MSN-NH_2 не впливали на позаклітинний синаптосомний рівень збуджуючого нейротрансмітера L-[^{14}C]глутамату і, отже, не викликали ексайтотоксичності. У флуоресцентних дослідженнях MSN-NH_2 деполяризували мембрану, демонстрували слабкі антиоксидантні властивості, зменшували спонтанну генерацію активних форм кисню, не змінюючи кількість H_2O_2 в нервових закінченнях. Модель Cd^{2+}/Pb^{2+}/Hg^{2+}-індукованої ексайтотоксичності була використана для оцінювання здатності MSN-NH_2 адсорбувати важкі метали. MSN-NH_2 не модулювали Cd^{2+}/Pb^{2+}/Hg^{2+}-індуковане підвищення позаклітинного синаптосомального рівня L-[^{14}C]глутамату.

Висновки. MSN-NH_2 не демонстрували ексайтотоксичних ознак, мали слабкі антиоксидантні властивості, і, тому, є біосумісними, не пом'якшували ексайтотоксичні ефекти ксенобіотичних важких металів і не адсорбували ці метали в біологічній системі.

Ключові слова: мезопористі наночастинки кремнезему із закріпленими аміногрупами, нейромодулювальні, мембранотропні, антиоксидантні властивості, ксенобіотичні важкі метали, глутамат, нервові закінчення кори головного мозку.